ISTANBUL UNIVERSITY –
JOURNAL OF ELECTRICAL & ELECTRONICS ENGINEERING

YEAR : 2007 (331 - 343)
VOLUME : 7
NUMBER : 1

ROBUST CONTROL OF UNIFIED POWER FLOW CONTROLLER (UPFC)

T. ALLAOUI M. A. DENAÏ M. BOUHAMIDA C. BELFEDAL

University of Science and Technology of Oran, Faculty of Electrical Engineering
BP 1505 El-Mnaouar, Oran, AlgeriaTel/Fax : +213 41 425509

[1]E-mail : allaoui_tb@yahoo.fr [2]E-mail : ma_denai@hotmail.com
[3]E-mail : m_bouhamida@yahoo.com [4]E-mail : bochradz@yahoo.com

ABSTRACT

This paper investigates control methods for the unified power flow controller in order to improve the stability of a power system hence providing security under increased power flow conditions. These include a direct PI controller with decoupling (PI-D), MIMO internal model control, multivariable GPC, multivariable GPC with decoupling algorithm (GPC-D) and adaptive fuzzy logic controls. The performances of the controllers are evaluated under different operating conditions of the power system. The results demonstrate that IMC, GPC, multivariable GPC-D and FLC are very effective in improving the transient power system stability and very robust against variable transmission line parameters.

Keywords: : *UPFC, PI controller, MIMO IMC controller, decoupling multivariable GPC with reference observation, decoupling fuzzy logic controller.*

1. INTRODUCTION

Flexible AC Transmission Systems (FACTS) are high power electronics based devices capable of altering voltage, phase angle and/or impedance at particular points in power systems [1]. Their fast response offers a high power system stability enhancement therefore preventing possible voltage collapse. Example of FACTS include the Unified Power Flow Controllers

(UPFC) which is capable of directing real and reactive power flows through a designated route and regulating the system voltage by providing fast reactive power compensation. Consequently the transmittable power capability of the transmission facilities can be utilized more efficiently.

A UPFC consists of two forced-commutated VSCs which are connected through a common dc link. One converter is shunt connected and the other is connected in series with the transmission line as illustrated by Fig. 1. The name Unified Power Flow Controller comes from the fact that it is possible for the device to control both transmitted active and

reactive power as well as the ac bus voltage at the point where shunt converter is connected (i.e. point A). The UPFC can provide different functions when the inserted series voltage v_c have different magnitude and phase angle. It will function as a pure voltage regulator if the inserted series voltage is in phase with the ac bus voltage. It will function as a pure series line

Received Date : 12.05.2006
Accepted Date: 01.02.2007

compensator if the inserted series voltage is perpendicular to the line current. It is also possible the UPFC to function as a phase angle regulator.
To improve the performance of the UPFC the interaction between the real and reactive power flow control system must be reduced [2]. Different control techniques for the UPFC system have been proposed [3-4].

In this paper MIMO internal model control (IMC), algorithm for decoupling multivariable systems based on generalized predictive control (GPC-D) and decoupling based on a fuzzy MIMO controller (FLC) are applied. The simulation results demonstrate superior performance and robustness of the system compared to a Proportional-Integral (PI) controller.

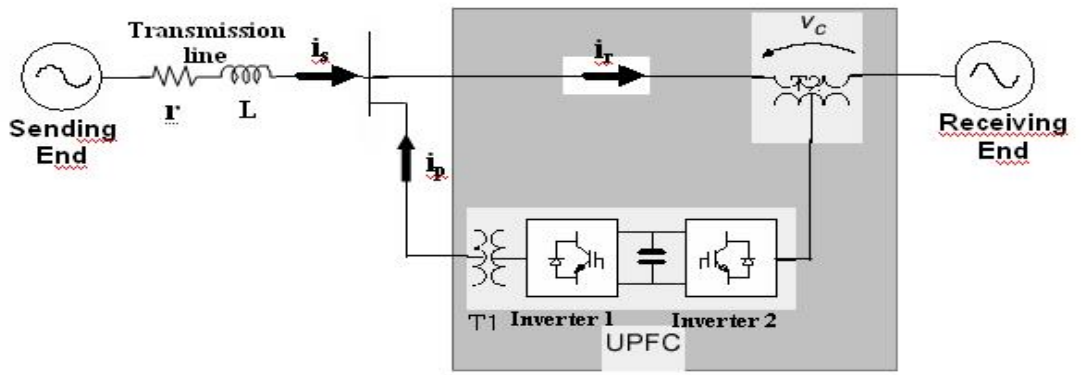

Fig.1 *Basic circuit configuration of a UPFC*

2. MODELLING OF THE UPFC

The equivalent circuit of a UPFC system is shown in Fig. 2 where the series and shunt inverters are represented by voltage sources v_c and v_p respectively. The transmission line is modelled as a series combination of resistance r and inductance L. The parameters r_p and L_p represent the shunt transformer resistance and leakage inductance respectively. The non linearities caused by the switching of the semiconductor devices, transformer saturation and controller time delays are neglected in the equivalent circuit and it is assumed that the transmission system is symmetrical.

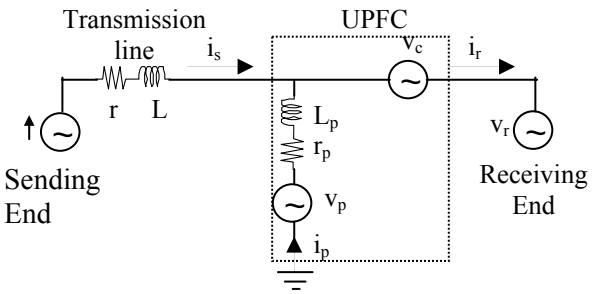

Fig. 2 *Equivalent circuit of UPFC system.*

By performing Park transformation, the current through the transmission line can be described by the following equations [3].

$$\frac{di_{sd}}{dt} = \omega i_{sq} - \frac{r}{L} i_{sd} + \frac{1}{L}(v_{sd} - v_{cd} - v_{rd}) \quad (1)$$

$$\frac{di_{sq}}{dt} = -\omega i_{sd} - \frac{r}{L} i_{sq} + \frac{1}{L}(v_{sq} - v_{cq} - v_{rq}) \quad (2)$$

where subscripts d and q denote the Park components of the currents and voltages.
Similarly, the shunt inverter can be described by

$$\frac{di_{pd}}{dt} = \omega i_{pq} - \frac{r_p}{L_p} i_{pd} + \frac{1}{L_p}(v_{pd} - v_{cd} - v_{rd}) \quad (3)$$

$$\frac{di_{pq}}{dt} = -\omega i_{pd} - \frac{r_p}{L_p} i_{pq} + \frac{1}{L_p}(v_{pq} - v_{cq} - v_{rq}) \quad (4)$$

Using the power balance principle and neglecting the inverter losses, the dc bus voltage can be described by [5]

$$\frac{dv_{dc}}{dt} = \frac{3}{2Cv_{dc}}\left(v_{cd} i_{rd} + v_{cq} i_{rq} - v_{pd} i_{pd} - v_{pq} i_{pq}\right) \quad (5)$$

3. CONTROLLER DESIGN

3.1. PI DECOUPLING CONTROL

The principle of this control strategy is to convert the measured three phase currents and voltages into d-q values and then to calculate the current references and measured voltages as follows [2]

$$i_{sd}^{*} = \frac{2}{3}\frac{(P^{*}.v_{sd} - Q^{*}.v_{sq})}{v_{sd}^{2} + v_{sq}^{2}} \quad (6)$$

$$i_{sq}^{*} = \frac{2}{3}\frac{(P^{*}.v_{sq} + Q^{*}.v_{sd})}{v_{sd}^{2} + v_{sq}^{2}} \quad (7)$$

Where the * superscript defines the reference qantities.

The power flow control is then realised by using properly designed controllers to force the line currents to follow their references. It is desired that the UPFC control system has a fast response with minimal interaction between the real and reactive power together with a strong damping of the resonance frequency.

In Fig. 3 is depicted the PI-based decoupling control system for the UPFC.

With reference to equations (1), (2),(3) and (4) the interaction between the current loops is caused by the ωL coupling term. Decoupling is achieved by feeding back this term and subtracting [4].
However, perfect decoupling is difficult to achieve with a PI-D controller due to the presence of time-delays and other non linearities in the UPFC system.

3.1.1. PERFORMANCE EVALUATION

The simulation is performed with MATLAB/SIMULINK software program. For each of the control systems mentioned above, simulation model is created which includes the required PWM.

The parameters of the simulation model are listed below [3].

$v_s = 220\,V \quad v_r = 220\,V \quad v_{dc} = 280\,V \quad f = 50\,Hz$

$r = 0.8\,\Omega \quad L = 10\,mH \quad r_p = 0.4\,\Omega \quad L_p = 10\,mH$

$C = 2000\,\mu F$

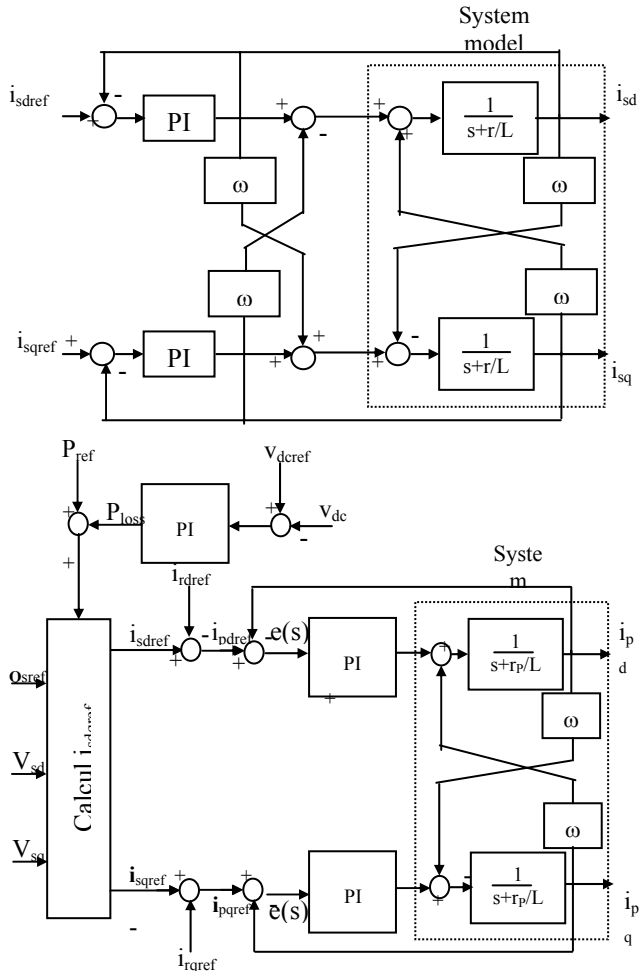

Fig. 3 *PI decoupling UPFC control system.*

Figures 4 and 5 shows the step response of PI decoupling control system .It can seen that the interaction between the real and reactive power in sending and receiving end, and between the isd and isq current and the system has a slower response.

Fig.7 presents the results for two cases which have the largest variations in line parameters compared with Fig.4 (a).

In test case1 the inductance of transmission line is increased by 25% compared with case 0.
In test case2 the inductance of transmission line is reduced by 25% compared with case 0.

It can seen from this Figure that robust stability and performance are not achieved with PI-D controller when the transmission line inductance is decreased or increased.

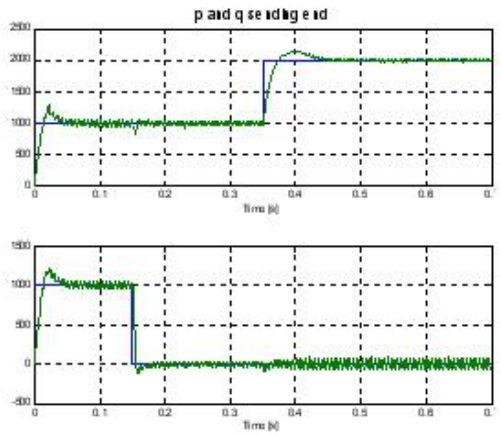

a) Ps and Qs Power

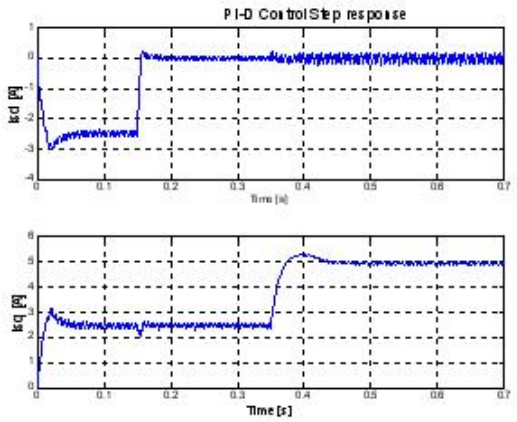

b) Isd and Isq Current

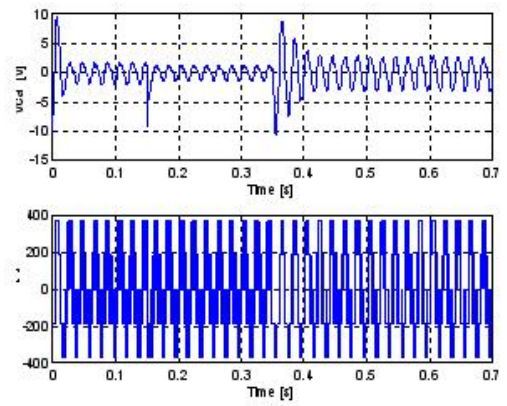

c) vca reference volage and vca voltage*

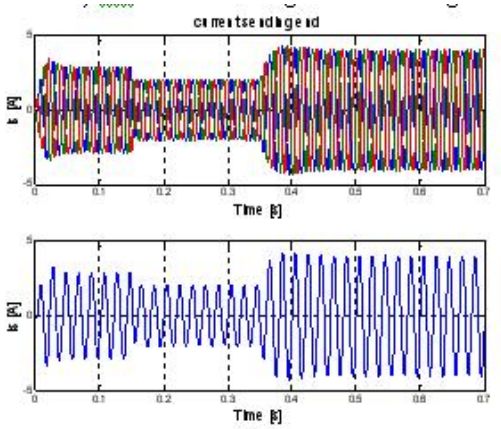

d) Current waveforms

***Fig.4** Simulation results of step responses with PI-decoupling in sending end*

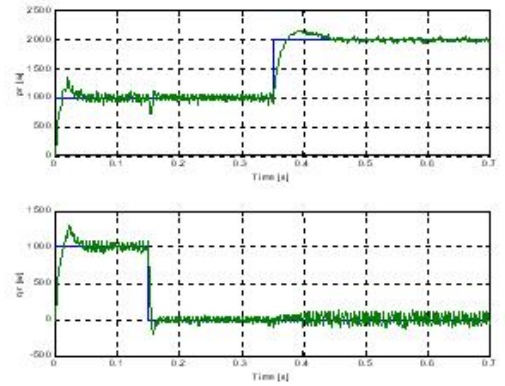

a) Pr and Qr Power

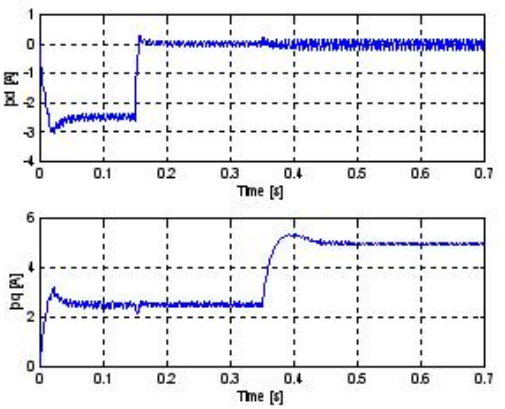

b) Ird and Irq Current

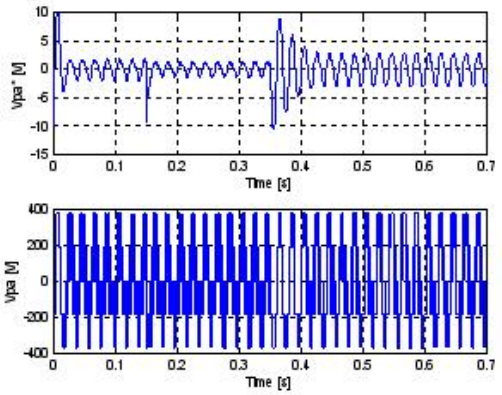

c) *vpa* reference voltage and vpa voltage*

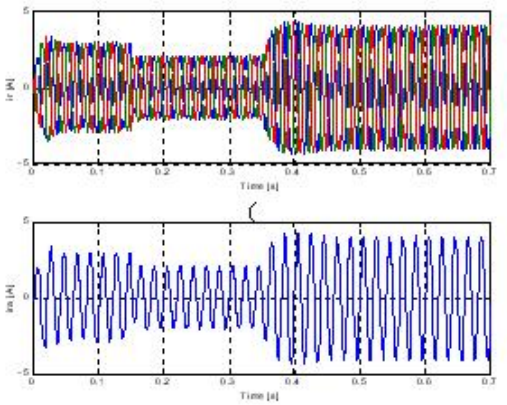

d) Current waveforms

Fig.5 *Simulation results of step responses with PI-decoupling in receiving end*

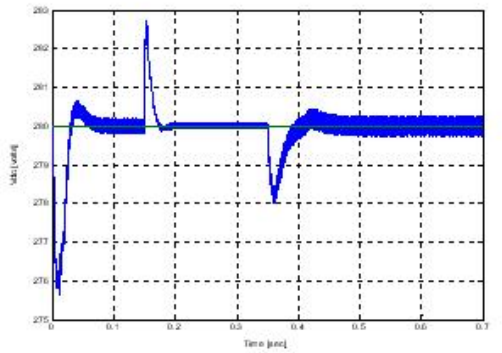

Fig.6 *DC Voltage*

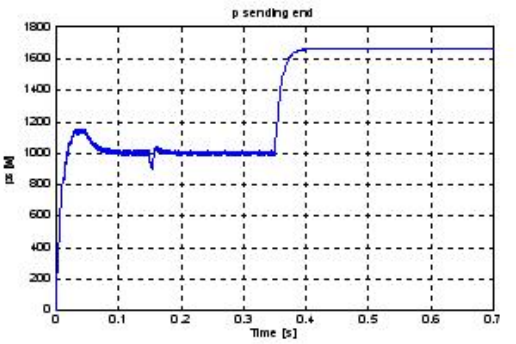

Case1 : L decreased by 25%

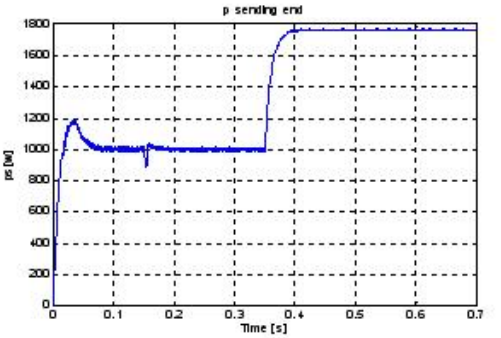

Case 2 : L increased by 25%

Fig.7 *Step responses under parameter changes*

3.2. IMC DESIGN

The basic architecture of a classical internal model controller (IMC) is illustrated by Fig. 8 [6]. A system model is placed in parallel with the actual system. The difference is used to adjust the command signal.

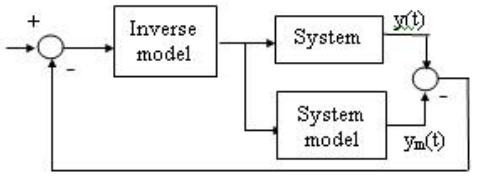

Fig. 8 *IMC structure*

An attractive feature of IMC is that it produces an offset-free response even when the system is subjected to a constant disturbance. Also, the closed-loop performance is directly related to simple controller parameters, which makes it very easy to tune the IMC controller. However, the order of the resulted controller, which is equivalent to the conventional feedback controller, is not necessarily high.

The concept of IMC [7] is illustrated originally came from of the fact that the complete control system includes the process model explicitly in addition to the controller. Fig.9-a show the block diagram of the inter model control system, where *C(s)* represents the IMC controller. However, by comparing Fig.9-b with classic feedback controller it is easy to find the relationship between the classic feedback controller K(s) and IMC controller C(s), that is,

$$K(s) = (1 - G(s)C(s))^{-1} C(s) \tag{8}$$

If the process G_M is stable and G is equal to G_M, the classical feedback system with controller K is internally stable if and only if C is stable. Therefore, the IMC can be implemented as the classic feedback controller. But the design of the IMC controller *C(s)* is much more simple, as will be shown later.

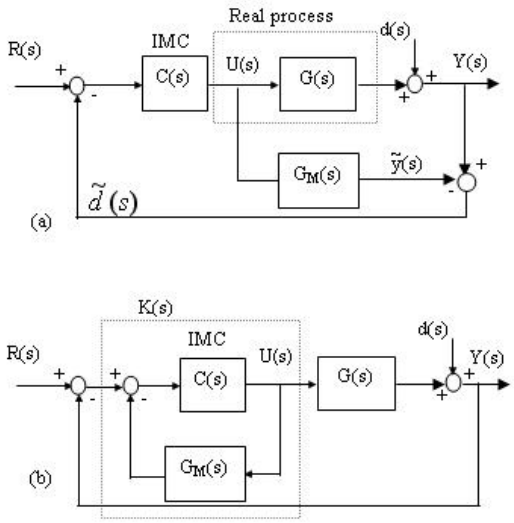

Fig 9.*Block diagram of IMC*

In order to investigate the closed-loop system stability and control performances, the sensitivity functions S(s) and T(s) are derived for the system shown in Fig.9-a as follows.

$$S(s) = \frac{y(s)}{d(s)} = \frac{1 - G(s)C(s)}{1 + C(s)[G_M(s) - G(s)]} \tag{9}$$

$$T(s) = \frac{y(s)}{r(s)} = \frac{G(s)C(s)}{1 + C(s)[G_M(s) - G(s)]} \tag{10}$$

In the special case that the plant model G(s) is an exact representation of the real plant $G_M(s)$,i.e., $G(s)=G_M(s)$, the sensitivity functions described in (9) and (10) will become

$$S(s) = 1 - G(s)C(s) \tag{11}$$

$$T(s) = G(s)C(s) \tag{12}$$

It can be clearly seen from (11-12) that the closed – loop system will be stable if the controller *C(s)* and the process *G(s)* are stable. The perfect control performance, with output y(s) tracking the reference r(s) instantly and not sensitive to any disturbance *d(s)*, can be achieved by setting controller *C(s)* equal to $G^{-1}(s)$. However, this perfect result can not be accomplished in reality due to several reasons.

- $G^{-1}(s)$ is improper, if *G(s)* is strictly proper,(e.g., the denominator order is higher than the numerator order) ;

- Existence of model uncertainty;

- $G^{-1}(s)$ can be unstable, if *G(s)* contain right – Nevertheless, with a few modification, good performance can be achieved easily according to the simple relationships between the sensitivity functions and controller as given in (8).

Therefore, if *G(s)* does not contain RHP zeros, feasible controller with good performance should be

$$C(s) = G^{-1}(s)\frac{\alpha^n}{(s + \alpha^n)} \tag{13}$$

where the positive integer n in chosen sufficiently large so that C(s) is proper, and α is a constant which determines the closed – loop control bandwidth.

The closed-loop system can be made arbitrarily robust simply by making α smaller.

If G(s) contains RHP zeros, the transfer function G(s) can be factorised as

$$G(s) = G_A(s)G_M(s) \tag{14}$$

where $G_A(s)$ is the allpass part of *G(s),* including all RHP zeros.

Then the stable controller with good performance can be obtained as (9)

$$C(s) = \tilde{G}^{-1}(s)\frac{\alpha^n}{(s + \alpha^n)} \tag{15}$$

With $\tilde{G}(s) = G_M(s)$

According to (14) or (15), it can be seen that the order of the IMC controller is also determined by

the order of the plant. A higher order plant will result in a more complex controller. However, it should be noted that the IMC thinking has been successfully used to design PI or PID controller in chemical applications. The reason is that many processes behave as a first order system in the low frequency range. In the high frequency range the pass filter included in the IMC controller. Thus it is sufficient to use a first order approximation model $\widetilde{G}(s)$ instead of G(s) when design the controller. If the order of the low-pass filter also chosen to be one, the first order model $\widetilde{G}(s)$ will give a first order feedback controller K(s), which should be equivalent to a PI controller.

The first order approximation of G(s) can be derived from the system equations(1)~(7).

As the two direct coupling functions $G_{11}(s)$ and $G_{22}(s)$ (refer to equation) have the same dynamic property, the low-pass filter is chosen as follows [8].

$$F(s) = \frac{\alpha}{s+\alpha} \tag{16}$$

Using equation (8), the equivalent classic feedback controller can be obtained, that is

$$K(s) = \left(1 - \widetilde{G}(s)\widetilde{G}^{-1}(s)\frac{\alpha}{s+\alpha}\right)^{-1} \widetilde{G}^{-1}(s)\frac{\alpha}{s+\alpha}$$

$$K(s) = \frac{\alpha}{s}\widetilde{G}^{-1}(s) \tag{17}$$

Furthermore, the step response of system. It can In order to verify the robustness of the designed controllers, different test cases have been done. Each test case has a different transmission line parameters, but the controller is fixed as designed for case0. Fig.6.2 presents the results for two cases which have the largest variations in line parameters compared with case0.

In test case1 the inductance of transmission line is increased by 25% compared with case0.

In test case2 the inductance of transmission line is reduced by 25% compared with case0.

3.2.1. PERFORMANCE EVALUATION

It can seen from Fig.10 that the minimal interaction between the real and reactive power that IMC controller show very similar performance in all the three cases. The robust stability and performance are achieved with IMC controller when the transmission line inductance is decreased or increased.

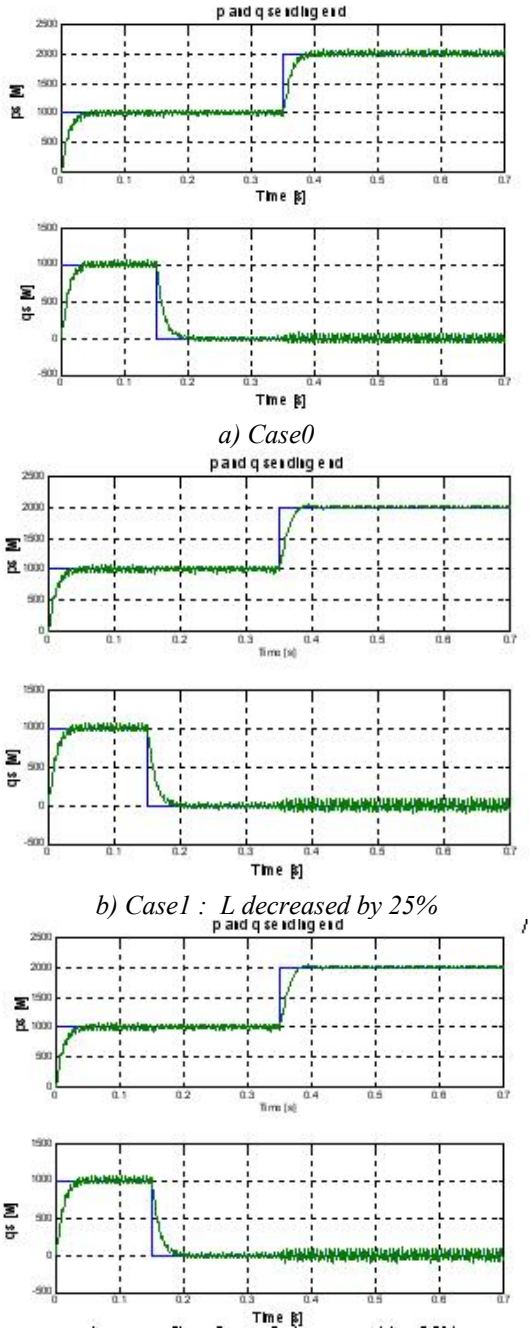

a) Case0

b) Case1 : L decreased by 25%

c) Case2 : L increased by 25%

Fig.10 *Simulation results of step responses with IMC control*

3.3. DECOUPLING GPC CONTROLLER

Generalized predictive control [9] seems to be attractive solution in process control, especially for multivariable systems. Multivariable GPC [10] takes into consideration interactions between loops what improves control performance. However, these controllers can not fully solve problems with interaction compensators to controllers can improve control [11].

Decoupling MIMO GPC usually has modified cost function and some decoupling algorithm [12]. Algorithm described here introduces additional error signals weighting. Error signal weights are evaluated from the filtered reference signals at each sample. When controller observes reference change in a control loop, it increases error weights in all other loops 'tightening' outputs on its references. That decreases interactions, which is shown through simulation study. Proposed algorithm is very simple to implement which makes it suitable for adaptive versions.

3.3.1. PROCESS MODEL

Let the controlled process be described by the discrete MIMO CARIMA model

$$A(z^{-1})\,y(k) = B(z^{-1})\,u(k-1) + \frac{\xi(k)}{\Delta} \quad (18)$$

where $u(k)$ represents control vector , $y(k)$ is the process output vector, $\xi(k)$ is a vector of uncorellated noise measurements with zero mean and $\Delta = 1 - z^{-1}$ is the backward difference. $A(z^{-1})$ and $B(z^{-1})$ are matrix polynomials in the backward shift operator.

$$A(z^{-1}) = I + A_1 z^{-1} + A_2 z^{-2} + \ldots + A_{np} z^{-nA} \quad (19)$$

$$B(z^{-1}) = B_0 + B_1 z^{-1} + B_2 z^{-2} + \ldots + B_{nB} z^{-nB} \quad (20)$$

Cost Function

Predictive control strategy minimises the following cost functio

$$J = \sum_{i=1}^{m} \left\{ r_i \sum_{j=1}^{N_2} [y_i(k+j) - w_i(k+j)]^2 + \lambda \sum_{j+1}^{N_u} \Delta u(k+j-1) \right\} \quad (21)$$

or in matrix form

$$J = [y - w]^T R[y - w] + \lambda \Delta u^T \Delta u \quad (22)$$

to find the future control vector which drives future process outputs to their respective reference values in a predefined horizon.

N_2, and N_u are the maximum and control horizons, λ is the control signal weight coefficient and R is the matrix of error signal weighting coefficients r_i

Control Law

The process output prediction is given by

$$\hat{y} = G\Delta\tilde{u} + f \quad (23)$$

where

$$G = \begin{bmatrix} g_0 & 0 & \cdots & 0 \\ \vdots & g_0 & \cdots & \vdots \\ g_{N-2} & \ddots & \cdots & 0 \\ g_{N-1} & g_{N-2} & \cdots & g_0 \end{bmatrix} \quad \text{and}$$

$$\hat{y} = [\hat{y}(k)\hat{y}(k+1)\cdots\hat{y}(k+N_2)]^T$$

$$\Delta\tilde{u} = [\Delta u(k-1)\Delta u(k)\cdots\Delta u(k+N_u-1)]^T$$

$$f = [f(k)f(k+1)\cdots f(k+N_2)]^T$$

Vector f defines the free model response and matrix G contains step response parameters [9-10]. The optimal control vector is found as

$$\Delta\tilde{u} = [I0\cdots0]\left[G^T RG + \lambda I\right]^{-1} RG^T(w - f) \quad (24)$$

Decoupling Control Strategy

The weighting matrix R is a diagonal matrix consisting of m sub-matrices R_i (i=1,...,m) and each R_i sub-matrix is diagonal with N_2 elements r_i [12] :

$$R = \begin{bmatrix} R_1 \cdots 0 \\ \vdots \ddots \vdots \\ 0 \cdots R_m \end{bmatrix} \qquad R_i = \begin{bmatrix} r_{i1} \cdots 0 \\ \vdots \ddots \vdots \\ 0 \cdots r_{iN2} \end{bmatrix}$$

$$r_{i1} = r_{i2} = \ldots = r_{iN2} = r_i$$

Matrix elements r_i weight the error signal, difference between the future output and its reference within the maximum horizon N_2.

Following a reference change (say, the j^{th} reference), the controller firstly increases r_i in all loops except in j^{th} , and then calculate optimal

control vector that would minimise the output deviation from its reference.

The weighting factors r_i are evaluated from

$$r_i = 1 + \sum_{\substack{j=1 \\ j \neq i}}^{m} \frac{K_{R_j}}{M(z^{-1})} \Delta\omega_j \qquad (25)$$

where $\Delta\omega_j$ is a reference change on j^{th} input., K_{R_j} is the maximum error weight in the j^{th} loop whose value depends on process parameters and can vary in broad range (0.1 – 1000) [11]. Higher values of K_{R_j} lead to better decoupling but in same time, too high K_{R_j} might produce slower reference tracking. $M(z^{-1})$ is a first order polynomial in the backward shift operator defined as $(1 - m_1 z^{-1})$, where m_1 defines the falling time of r_i. Value of m_1 must be chosen to encompass entire transient dynamics of diagonal transfer function and usually, it has value between 0.8 and 0.95 [12].

Lower m_1 means faster decreasing of r_i witch implies worse interaction compensation and vice versa. On the other hand, too high m_i might cause problems with distribution compensation [13].

3.3.2. PERFORMANCE EVALUATION

The parameters of the proposed decoupling controller are the following:

$$\begin{bmatrix} A_1(z^{-1}) & 0 \\ 0 & A_2(z^{-1}) \end{bmatrix} \begin{bmatrix} y_1(k) \\ y_2(k) \end{bmatrix} = \begin{bmatrix} B_{11}(z^{-1}) & B_{12}(z^{-1}) \\ B_{21}(z^{-1}) & B_{22}(z^{-1}) \end{bmatrix} \begin{bmatrix} u_1(k-1) \\ u_2(k-1) \end{bmatrix}$$

where y_1 is a i_{sd} or i_{pd} currents, y_2 is a i_{sq} or i_{pq} currents, u_1 is a control signal (v_{cd} or v_{pd}), u_2 is a control signal (v_{cq} or v_{pq}). The polynomials A_1 , A_2 , B_{12} , B_{22} , B_{21} , B_{22} are given by

$$A_1 = 1 - 0.001068\, z^{-1} + 0.4493\, z^{-2}$$
$$A_2 = 1 - 0.001068\, z^{-1} + 0.4493\, z^{-2}$$
$$B_{11} = -0.2766\, z^{-1} + 0.1663\, z^{-2}$$
$$B_{12} = 0.2478\, z^{-1} + 0.1853\, z^{-2}$$
$$B_{21} = -0.2478\, z^{-1} - 0.1853\, z^{-2}$$
$$B_{22} = -0.2766\, z^{-1} + 0.1663\, z^{-2}$$

Fig.11 shows the step response of multivariable GPC system .It can seen that the interaction between the real and reactive power, and between the i_{sd} and i_{sq} current and the system has a slower response.

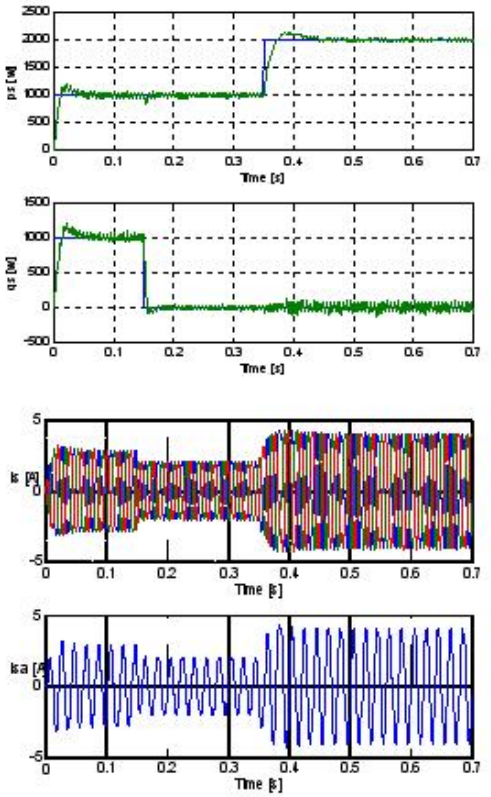

Fig. 11 *Simulation results of step responses with multivariable GPC*

In order to verify the robustness of the designed controllers, different test cases have been done. Each test case has a different transmission line parameters, but the controller is fixed as designed for case 0. Fig.12 presents the results for two cases which have the largest variations in line parameters compared with case 0.

In test case1 the inductance of transmission line is increased by 25% compared with case 0.

In test case2 the inductance of transmission line is reduced by 25% compared with case 0.

It can seen from Fig.12 that the minimal interaction between the real and reactive power that decoupling multivariable systems based on generalized predictive control (GPC-D) show very similar performance in all the three cases. The robust stability and performance are

achieved with GPC controller when the transmission line inductance is decreased or increased.

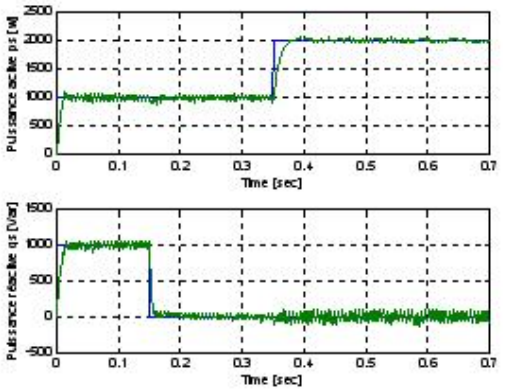

Case 0

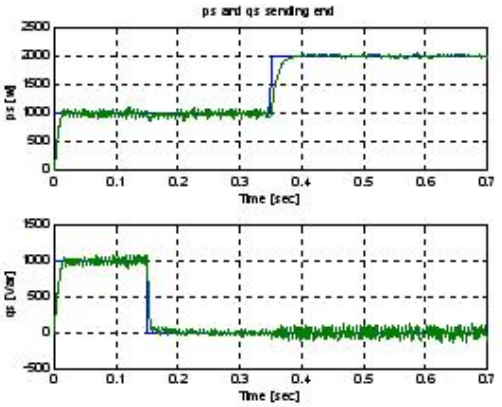

Case 1 : L decreased by 25%

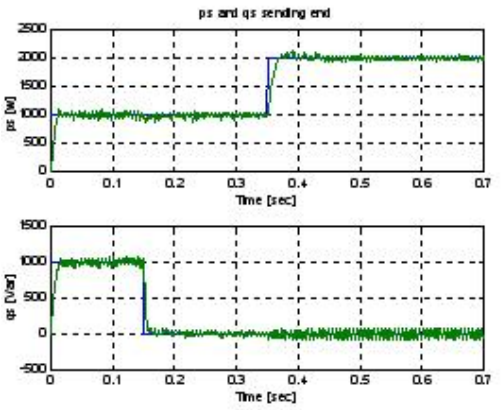

Case 2 : L increased by 25%

Fig. 12 *Simulation results of step responses with decoupling multivariable GPC*

3.3. DECOUPLING FLC CONTROLLER

The fuzzy decoupling controller has a PI (Proportional Integral) structure as illustrated by Fig. 13

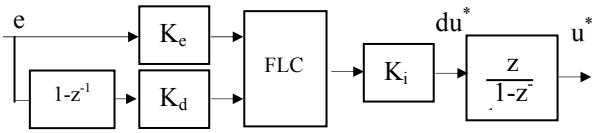

Fig. 13 *Structure of the PI fuzzy controller*

or ε is the system error , $\Delta\varepsilon = \varepsilon_K - \varepsilon_{K-1}$.
The typical PI control law in its standard form is:

$$\Delta u_K = K_P.(\varepsilon_K - \varepsilon_{K-1}) + K_P \frac{T}{\tau_I}\varepsilon_K$$

Or k_p the proportional gain and τ_i the integral gain chosen, Δu_k is the increment of control. Parameters k_p and τ_i are chosen according to predicates associated to ε and $\Delta\varepsilon$.

In Fig. 14 is depicted the FLC-based decoupling control system for the UPFC [14].
The FLC inputs are the errors signals (e_1= i_{sd}^*- i_{sd}) and (e_2 =i_{sq}^*- i_{sq}). The outputs are v_{cd} and v_{cq}.

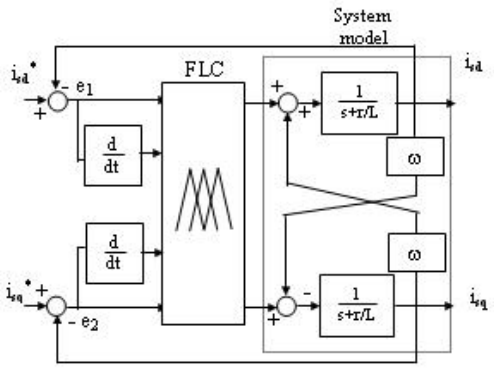

Fig. 14 *FLC decoupling UPFC control system*

The universe of discourse for the input variables (error and error change) are defined by two fuzzy subsets {N, P} where N (Negative) and P (Positive) are linguistic variables. The universe of discourses for v_{cd} and v_{cq} voltages are defined by the fuzzy subsets {N, Z, P}

The membership functions for the input and output variables are of triangulaire shape and are represented in Fig. 15 and 16 respectively.

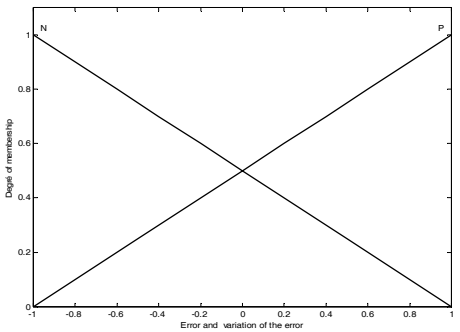

Fig. 15 *Membership functions of e and of* Δe

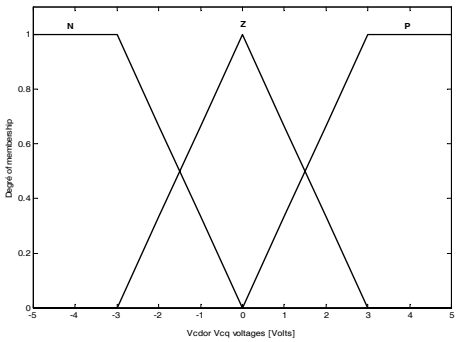

Fig. 16 *Membership functions of* Δu

The fuzzy inference rules are in the form
IF e_1 is N AND Δe_1 is P AND e_2 is P AND Δe_2 is P THEN v_{cd} is Z AND v_{cq} is N
The decoupling strategy is performed by the rule base matrix given by Table 1.

e_1	Δe_1	e_2	Δe_2		v_{cd}	v_{cq}
N	N	N	N		P	P
N	N	N	P		P	Z
N	N	P	N		P	Z
N	N	P	P		P	N
N	P	N	N		Z	P
N	P	N	P		Z	Z
N	P	P	N		Z	Z
N	P	P	P		Z	N
P	N	N	N		Z	P
P	N	N	P		Z	Z
P	N	P	N		Z	Z
P	N	P	P		Z	N
P	P	N	N		N	P
P	P	N	P		N	Z
P	P	P	N		N	Z
P	P	P	P		N	N

3.4. PERFORMANCE EVALUATION

Fig. 17 shows the step responses of active and reactive powers.

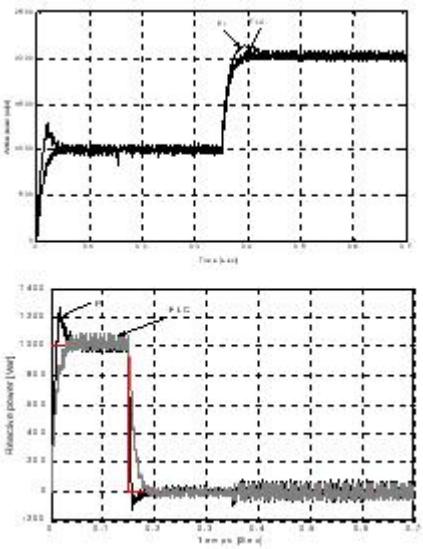

Fig. 17 *Step responses of* P_s *and* Q_s

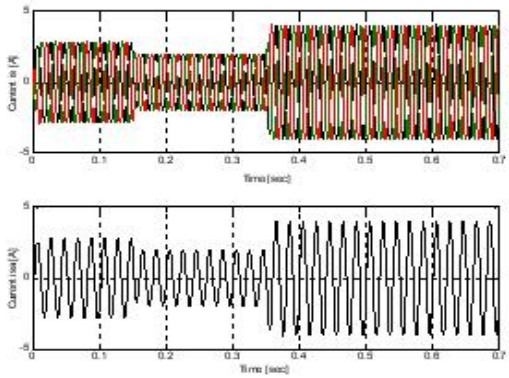

Fig. 18 *Currents waveforms*

In order to assess the robustness of the controller with respect to line inductance variations, different test cases have been performed. Each test case has a different transmission line parameters, but the controller is fixed as designed for case 0. Fig. 19 presents the results for two cases. In test case 1 the inductance of transmission line is reduced by 25% while in test case 2 the inductance of transmission line is reduced by 25% compared with case 0. It can seen from Fig. 17 that interaction effect is very small and does not affect the controller performance which demonstrate the robustness of the decoupling FLC controller.

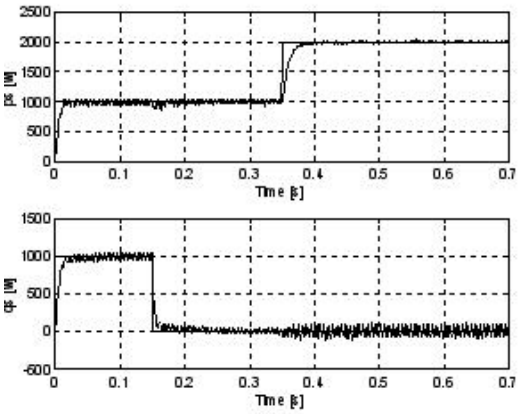

Case 0

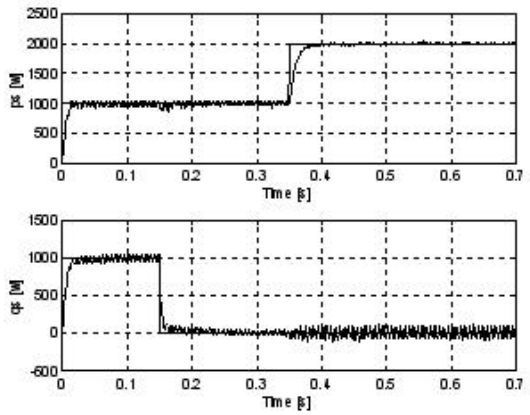

Case 1 : L decreased by 25%

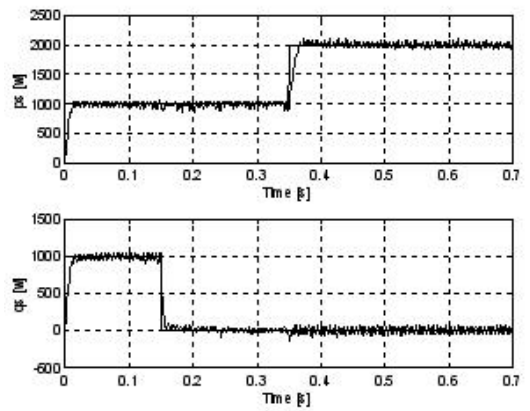

Case 2 : L increased by 25%

Fig. 19 *Robustness test of MIMO FLC*

4. CONCLUSIONS

In this paper a four controllers (PI, IMC, GPC-D, FLC-D) has been evaluated for UPFC-based power flow compensation. The simulation results show that improved performance has been achieved by these controllers as compared to PI control. PI decoupling control can cause large interactions between the current loops and a of the transmission system are actually known. IMC, GPC-D and FLC-D controllers provides better performance and robustness even under large transmission line parameter changes. For any controllers more simulation results will be presented and discussed by considering other operating conditions of the UPFC system together with a comparative study between the proposed control strategies.

REFERENCES

[1] Ying Jiang,"Active and Reactive Power Control For Transmission Systems With Voltage Source Converters", 1997.

[2] Yu Q , Round S D, Norum L, Undeland T M, 1995,"A new control strategy for a unified power flow controller", *Proc. Of European Power Electronics Conference*, 2, 901 – 906

[3] Yu Q, Round S D, Norum L, Undeland T."Dynamic Control of Unified Power Flow Controller", *IEEE*, 1996.

[4] Papic, Zunko, D.Povh, Fellow, "Basic Control of Unified Power Flow Controller ", *IEEE Transactions on Power systems*,vol.12 ; N°4,November 1997.

[5] Yu Q , Round S D, Norum L, Undeland T M, "Performance of a Unified Power Flow Controller Using a d-q Control System"", *to be published at Proc. Of IEE AC/DC transmission conférence London*, 1996.

[6] Jean Marie FLAUS , *Régulation industrielle, chapitre 4, régulateur à modèle interne*, Hermes, pp.115 – 139, 1994

[7] Garcia, C.E. and M.Morari, ''Internal Model Control 2. Design Procedure for Multivariable Systems'' *Ind. Eng. Chem. Process Des. Dev*., 24, pp 472-484, 1985.

[8] T. Allaoui, M. A. Denaï , Robust Internal Model Control of UPFC-Based Power Flow Compensation, *conférence sur le genie électrique* CGE'04, EMP 25-26 decembre 2001.

[9] D. W. Clarke, ''Application of Generalized Predictive Contol-Part I and II'', *Automatica,* 23(2), 1987, p.p 137 – 160.

[10] D. W. Clarke, ''Application of Generalized Predictive Control to industrial processes'', *IEEE Control System Magazine*, 8, 1988, p.p 49 - 55.

[11] Chai T., Mao K., Qin X., ''Decoupling design of multivariable generalized predictive control'', IEE Proceedings on Control Theory & Applications, 1994. Vol 141, No.3, pp. 197-201.

[12] Bego O., Peric N., Petrovic I., ''Decoupling Multivariable GPC with Reference Observation'', *Proceedings of the 10th Mediterranean Electrotechnical Conference - MELECON* 2000, Cyprus.

[13] T. Allaoui, M. A. Denaï, M. Bouhamida, ''Decoupling Multivariable GPC Control of UPFC-Based Power Flow Compensation'', *10th International Conference EPE-PEMC* 2002, Zegreb-Croutia.

[14] M A. Denaï, T. Allaoui, ''Adaptive fuzzy Decoupling of UPFC-Power Flow Compensation'', *Straffordshires University UK, 37th UPEC* 2002, 9-11 September

BIOGRAPHIES

Tayeb Allaoui received his engineer degree in electrical engineering from the Ibn Khaldoun University of Tiaret in 1996 and his master degree from the University of Science and Technology of Oran in 2002. His is currently a lecturer at the Ibn Khaldoun University of Tiaret, Algeria. His research interests include intelligent control of power systems and FACTS, Active filter and reneweable energies.

Mouloud Denaï received the engineer degree in electrical engineering from Ecole Polytechnique of Algiers in 1982, the PhD in Control Engineering from the University of Sheffield, UK in 1988. Currently, he is a Professor in automatic control at the university of science and technology of Oran, Algeria. His research interests are in system modeling and control using soft-computing techniques.

Bouhamida Mohamed (Dr, Ing), 1956 received hisBachelor in Electronic Engineering in 1982 from the University of Science and Technology of Oran (Algeria) and his master in Automatic Control Engineering fromENSET of Oran in 1992. He is currently associate professor at the University of Science and the Technology of Oran. His main field of interestare robust control, adaptive control in power systems.

Cheikh Belfedal was born in Sougueur Algeria, in 1964. He received master degrees in electrical engineering from Tiaret University, Algeria, in 1996. Since 1996, he has been with the Department of Electrical Engineering, Tiaret University. He was a research assistant professor. His fields of interest are control of electrical machines, power converters, modelling and control of large wind turbines.